Characterization of Compositional Heterogeneity in Chemically Amplified Photoresist Polymer Thin Films with Infrared Spectroscopy

Shuhui Kang, Bryan D. Vogt,‡ Wen-li Wu, Vivek M. Prabhu,* David L. VanderHart, Ashwin Rao, and Eric K. Lin

Polymers Division, National Institute of Standards and Technology (NIST), 100 Bureau Drive, Gaithersburg, Maryland 20899

Karen Turnquest

SEMATECH, 2706 Montopolis Drive, Austin, Texas 78741

ABSTRACT: We demonstrate a general approach to characterize compositional heterogeneity in polymer thin films using Fourier transform infrared (FTIR) spectroscopy. Polymer films with varying degrees of heterogeneity were prepared using a model chemically amplified photoresist where a photoacid catalyzed reaction-diffusion process results in the formation of methacrylic acid (MAA) rich domains. Within these domains, the carboxylic acid groups dimerize through hydrogen bonding. FTIR measurements of the relative fraction of hydrogen-bonded vs free carboxylic groups are used to quantify the degree of compositional heterogeneity. The FTIR data from compositionally homogeneous systems, statistical copolymers, and polymer blends follow the expected linear dependence of the relative hydrogen-bonded fraction with composition. For the chemically amplified photoresist system, the FTIR data deviate substantially from that of the homogeneous distribution. Furthermore, parameters describing the size of the heterogeneity can be determined from a solid sphere model of the deprotected regions catalyzed by the diffusing photoacid. The degree of the spatial heterogeneity varies with changes in the photoacid concentration, reaction conditions, and initial copolymer composition. Increased nonreactive comonomer content decreases the degree of heterogeneity by reducing the hydrogen-bonding efficiency, which is consistent with the dilution of MAA groups.

1. Introduction

Lithographic imaging for the fabrication of modern microelectronics devices is enabled by chemically amplified photoresists.[1] In this process, an optical image is converted into a chemical latent image through a thermally activated reaction-diffusion process involving a photoinitiated acid catalyst. Each photoacid can participate in hundreds of reactions as it diffuses during the post exposure bake (PEB); hence, the effect of a single photon absorption is amplified.[2,3] This chemical image is developed with aqueous base to reveal the final physical features. The drive to fabricate ever smaller feature dimensions has led to increasingly stringent requirements on the photoresist.[1,4] Line edge roughness (LER), a metric of the feature quality, is a major limiting factor for sub-50-nm photolithography. LER is believed to result from the heterogeneous distribution in the deprotection product at the line edge of the latent image. The optical image quality of the exposure and the distribution of the subsequently generated photoacid catalysts is a key factor to LER.[5−9] Schmid et al.[10,11] modeled this process and showed that the reaction-diffusion of photoacid generates a heterogeneous distribution in deprotected monomer. This heterogeneous deprotection distribution results in local differences in solubility in the developer solution, where highly deprotected chains dissolve and those with insufficient deprotection remain in the film.[12] Simulations of Houle et al. yield similar conclusions.[13,14] In addition, this heterogeneous structure is described in a percolation model used to simulate the dissolution behavior of photoresists film.[15−19]

A quantitative measure of the degree of heterogeneity in the deprotection reaction product is needed to identify and enable design strategies to reduce materials sources of LER. Direct experimental observation of the degree of heterogeneity is difficult because of the small size scale and the limited contrast between protected and deprotected chains. Several measurements indirectly observe the degree of heterogeneity in chemically amplified photoresists. Stewart et al. observed differences between protected and deprotected regions in a scanning electron microscope (SEM) by overcoming the limited electron contrast between the components by selective staining of the deprotected regions with a heavy metal.[20] However, these measurements could not resolve the nanometer scale structure and could only observe larger scale reaction−diffusion.[20] Dragnea et al. used near-field Fourier transform infrared (FTIR) spectroscopy to directly observe the chemical image produced by a patterned photomask. However, the resolution was insufficient to observe the diffusion of single photoacids or distinguish between chemically different regions.[21] The shape and size of the deprotection reaction-diffusion path in a model partially deuterated photoresist was determined using small-angle neutron scattering (SANS).[22] The deprotection process does not result in hard spheres, but rather "fuzzy blobs" with characteristic fractal dimension.[22] Despite the success of SANS in determining the deprotection volume from a single photoacid, this technique is not widely utilized because it requires deuterium substitution

Scheme 1. Chemical Structures of Three Photoresists Used in This Study: Left, PMAdMA; Middle, P(MAdMA$_{50}$-*co*-GBLMA$_{50}$); Right, P(MAdMA$_{41}$-*co*-GBLMA$_{59}$)
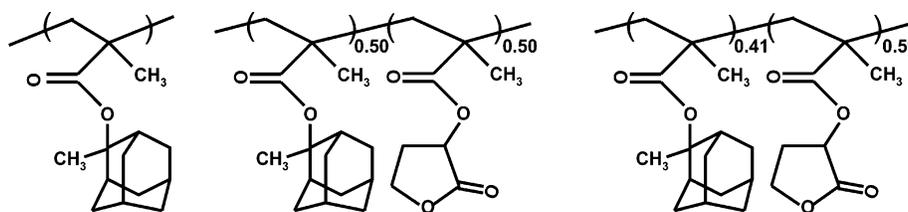
Table 1. Polymer Characteristics

polymer	M_w	M_w/M_n	T_g (°C)
PMAdMA	8800	1.18	>210
P(MAdMA$_{50}$-*co*-GBLMA$_{50}$)	12 800	1.67	161.9
P(MAdMA$_{41}$-*co*-GBLMA$_{59}$)	11 505	1.3	171.5

Scheme 2. Acid-Catalyzed Deprotection of PMAdMA

of the hydrogen atoms on the protecting groups and the limited availability of the instrumentation.

In this work, we develop a method to characterize the degree of heterogeneity in thin polymer films using FTIR on materials that exhibit hydrogen bonding. Chemically amplified photoresists are a good model system because the degree of heterogeneity is a critically important parameter for their performance. We investigate model 193 nm photoresists based on poly(methyl-adamantyl methacrylate) (PMAdMA), which upon complete deprotection forms poly(methacrylic acid) (PMAA). Carboxyl groups are well-known to form dimers that induce a band shift in C=O IR spectra relative to the monomer state. This feature has been used previously to characterize the interaction in polymer blends and layer-by-layer structures.[23,24]

Here, the carboxyl dimerization is utilized to characterize the structure formed by the acid-catalyzed deprotection reaction. Since hydrogen bonding (dimer) can only occur with adjacent C=O groups and the films are processed well below the glass transition, the local distribution in chemical composition generated by deprotection reaction can be deduced from the ratio of hydrogen bonded to free C=O groups. As a reference point, we use the fraction of hydrogen-bonded C=O groups when the sites are randomly distributed. If the measured fraction exceeds this limit, dimer clusters are expected and the positive deviation from the homogeneous limit is indicative of the degree of heterogeneity. The nonreactive comonomer content in photoresist polymers are necessary to control dose sensitivity, development, etch resistance, and transparency.[1] Here we demonstrate how the nonreactive comonomer content also reduces the degree of heterogeneity using a series of model copolymers. These results can help understand correlations between compositional heterogeneity and the roughness observed upon the dissolution[25] (development) of resists in aqueous bases, as well as provide information about the degree of heterogeneity in other thin film systems such as polymer blends and nanocomposites.

2. Experimental Section

2.1. Polymer Characteristics. We used three different model photoresist polymers based upon poly(methyladamantyl methacrylate) (PMAdMA). The PMAdMA homopolymer and a copolymer P(MAdMA$_{41}$-*co*-GBLMA$_{59}$) containing 59 mol % of the nonreactive α-γ-butyrolactone methacrylate (GBLMA) were provided by DuPont Electronics Polymers. A second copolymer containing 50 mol % GBLMA (P(MAdMA$_{50}$-*co*-GBLMA$_{50}$)) was supplied by AZ Electronics. The chemical structures of the three polymers are shown in Scheme 1 and their characteristics are listed in Table 1. The acid catalyst for the deprotection reaction is produced from a photoacid generator (PAG), triphenylsulfonium perfluorobutane-

sulfonate (TPS−PFBS), under UV exposure. The photoacid concentration generated from UV was calculated from exposure dose and PAG loading in the sample.[26] The photoacid-catalyzed deprotection reaction is shown in Scheme 2.
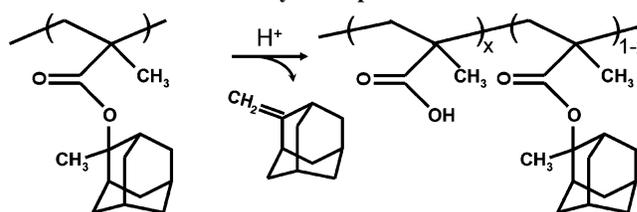
2.2. Sample Preparation. Films were prepared from solutions containing one photoresist polymer and PAG in cyclohexanone by spin-coating on double side polished silicon wafers at 209 rad/s (2000 rpm) with an acceleration rate of 105 rad/s^2 (1000 rpm/s) for 60 s. The samples were then baked at 130 °C for 60 s to remove residual casting solvent. The PAG was activated using a 248 nm broadband UV lamp. The exposed samples were then transferred to a preheated hot-plate for postexposure baking (PEB). The details about the sample preparation can be found in a previous publication.[26] To study the behavior of deprotection at very low extents of reaction, samples were also prepared on CaF$_2$ windows following the same procedure. To avoid issues with heat transfer, the PEB for the films on the CaF$_2$ windows were performed with the films facing down.

2.3. FTIR Spectroscopy. Transmission IR spectra were obtained with a Nicolet NEXUS 670 Fourier transform infrared (FTIR) spectrometer and analyzed with OMNIC software. A resolution of 8 cm^{-1} was used and 128 scans were averaged to improve the signal-to-noise ratio. The deprotection level is defined as the molar ratio of the reacted MAdMA group to the total MAdMA group in the film. The quantification of deprotection level was based on the CH$_3$ bending band (1360 cm^{-1}) for PMAdMA and C−O stretching band (1260 cm^{-1}) for the two copolymers.[26]

3. Results and Discussion

3.1. Free and Hydrogen-Bonded C=O in PMAdMA. A partially deprotected PMAdMA film can be treated as a binary system consisting of MAdMA (unreacted) and MAA (reacted) groups. For this system, there are three C=O peaks in the IR spectra located at approximately 1740, 1720, and 1700 cm^{-1}. The central peak (1720 cm^{-1}) results from the C=O in the unreacted PMAdMA polymer. The location of this band does not change with deprotection reaction. Therefore, this background "C=O" spectra can be removed by subtracting the spectra of the unreacted PMAdMA polymer based on its deprotection level. The resulting spectra in this region are solely from the carboxyl group in MAA. There are two main peaks in the IR spectrum for PMAA. The peak at higher wavenumber belongs to the free C=O, while the lower one belongs to hydrogen-bonded C=O, which arises from carboxyl dimers.[24,27] The relative intensity of these two peaks reflects the state of aggregation of carboxyl groups because the dimer can only form when two MAA groups are close enough to hydrogen bond. The typical proton donor to acceptor distance is between 1.5
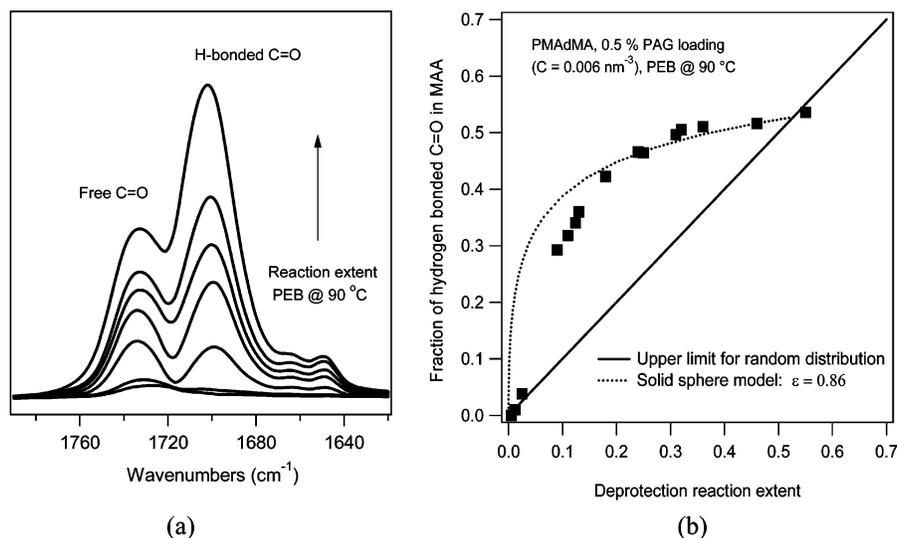
Figure 1. (a) Evolution of C=O stretching bands of MAA groups with reaction extent in PMAdMA samples. (b) Change of fraction of hydrogen-bonded C=O in MAA groups with deprotection reaction extent.

and 2.2 Å.[28] When another MAA group is not available, a free C=O is observed due to an absence of a proton donor.

Figure 1a shows the IR spectrum of MAA in a partially deprotected PMAdMA film with different extents of reaction. If we define a ratio of the hydrogen-bonded C=O to the total C=O in MAA, F_{bond}, we can obtain a continuous change of this ratio with the extent of reaction of the film (Figure 1b). Here, F_{bond} is calculated from the area under the IR peaks corresponding to hydrogen bonded and free C=O, A_{free} and A_{bond}, respectively. With an absorptivity ratio of 1.6 between free and hydrogen-bonded C=O,[24] the fraction of hydrogen-bonded C=O is given by

$$F_{bond} = (A_{bond}/1.6)/(A_{free} + A_{bond}/1.6) = \\ 1/(1 + 1.6\,A_{free}/A_{bond}) \quad (1)$$

In this analysis, we have neglected hydrogen-bonding between the photoacid and the carboxylic acid group.[26] However, the photoacid is a strong hydrogen donor and readily hydrogen bonds with MAA. If we assume that the photoacid is completely bonded with MAA groups, the contribution of the photoacid to F_{bond} is equal to its molar concentration in the photoresist. Although the maximum correction needed to account for the photoacid hydrogen bonding is negligible at low photoacid concentrations, this correction is applied to all the data unless specifically indicated otherwise.

3.2. Analysis Framework for Degree of Heterogeneity. The degree of heterogeneity within the film is defined relative to the ideal homogeneous structure with a random distribution of components. For a binary system A (MAA) and B (MAdMA), if we assume that the MAA groups are randomly and uniformly distributed for any given extent of reaction ϕ [$\equiv A/(A + B)$], the probability of finding a pair of A (MAA) groups is ϕ^2. Similarly, the probability of finding other pairs AB, BA, and BB are $\phi(1 - \phi)$, $(1 - \phi)\phi$ and $(1 - \phi)^2$, respectively. Since the bonded carbonyl exists only in AA pairs (MAA pairs), the ratio of the bonded to total C=O (free and bonded) F_{bond} is given by

$$F_{bond} = 2\phi^2/[2\phi^2 + \phi(1 - \phi) + (1 - \phi)\phi]\epsilon = \epsilon\phi \quad (2)$$

where the "ϵ" is the average efficiency of hydrogen bonding

for each MAA pair. The efficiency for two adjacent MAA group to dimerize should be less than 100%, i.e., $\epsilon < 1$, because hydrogen bonding has an orientation dependence that should not always be satisfied. The value of ϵ will be determined in a later section. Equation 2 shows a linear dependence of F_{bond} with composition when the system is perfectly mixed. In contrast, deviations from this linear dependence (eq 3) signify a degree of heterogeneity (DH) that may be defined as

$$DH = F_{bond} - \epsilon\phi \quad (3)$$

To test the scaling of F_{bond} with ϕ, we reexamined the data of Lee and co-workers for polymer blends of poly(ethylene-*co*-methacrylic acid) (EMAA) and poly(vinyl methyl ether) (PVME), which form miscible blends at elevated temperature.[24] Similar to our data in Figure 1a, the IR spectra for these blends exhibits two distinct C=O stretching bands corresponding to free and hydrogen-bonded MAA groups. Their data (Table 1 and also Figure 15)[22] have been plotted in Figure 2 for several different copolymer compositions. F_{bond} for the blends increases linearly with MAA concentration. However, we find that F_{bond} is larger than that expected from the randomly homogeneous model. This discrepancy could result from crystallization of the ethylene segments, which leads to heterogeneities that are copolymer dependent due to differences in the ethylene sequence length, but relatively independent of the PEMAA concentration. Lee and co-workers found that crystallization of the ethylene segments was enhanced by decreasing the MAA content. This observation is consistent with the copolymer dependence on the deviations from the theoretical line in Figure 2. For the copolymer with the greatest MAA and thus the least crystallizable ethylene, the data are very close to the upper limit of the theoretical prediction for a homogeneous distribution.

3.3. Quantification of the Heterogeneous Structure–Solid Sphere Model. With this framework, the FTIR data points in Figure 1b are well above the reference line, $F_{bond} = \phi$, confirming that a heterogeneous structure exists in the partially deprotected PMAdMA film. To quantify the dimensions of the heterogeneous regions, a model of the form of the deprotection reaction path induced by the diffusing acid is needed. Although SANS measurements demonstrate that the deprotection path is fractal in nature,[22] we simplify the analysis through the use of
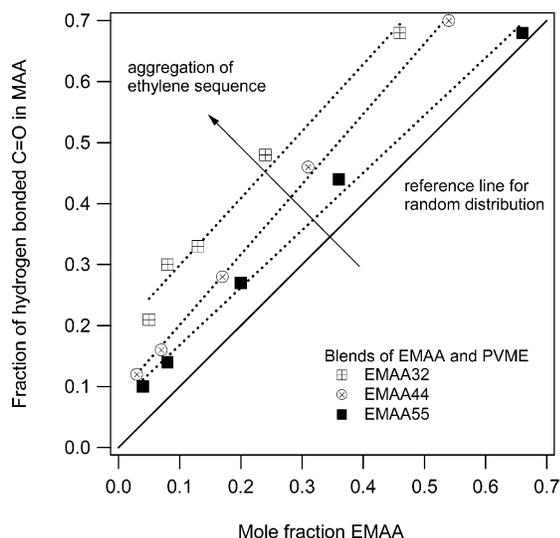
Figure 2. Analysis of the FTIR data (Figure 15) of Lee et al. EMAA32, EMAA44 and EMAA55 correspond to three different poly(ethylene-*co*-methacrylic acid) copolymers containing 32%, 44%, and 55% by weight of MAA, respectively. The *x*-axis corresponds to the mole fraction of MAA in the blends according to literature. The solid line is a reference to the expected dependence based on a random distribution ($F_{bond} = \phi$).
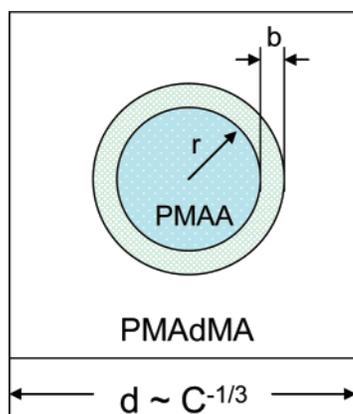
Figure 3. Schematic of the solid sphere model comprised of the core of radius *r* and shell of thickness *b*. The shaded region represents the PMAA domains produced by reaction. The boxed region corresponds to the average volume per photoacid related to the inverse photoacid concentration.

a solid sphere model to estimate the dimensions of the deprotection volume in the PMAdMA films. In this model, we assume that hydrogen-bonded C=O are confined inside the sphere volume (V_c), while the sphere surface (A_s) is decorated by free C=O as shown in Figure 3.

The sphere is characterized by an inner radius (r) and thickness (b) of the outer layer. The outer layer thickness ($b = 0.49$ nm) is determined by the MAA molecular repeat unit size in which $b = (M/\rho N_A)^{-1/3}$ with MAA molecular weight ($M = 86$ g mol^{-1}), density ($\rho = 1.19$ g/cm^3) and Avogadro's constant (N_A). The analysis here is only valid in the limit where the volumes of single photoacid catalyzed deprotected regions do not overlap.

Given this model and the initial photoacid concentration before PEB, we derive an expression for F_{bond} as a function of ϕ. The macroscopic average deprotection level, ϕ, defined by the fraction of MAdMA converted to MAA is quantified from the FTIR measurements.[26] The total volume of MAA (V_{MAA})
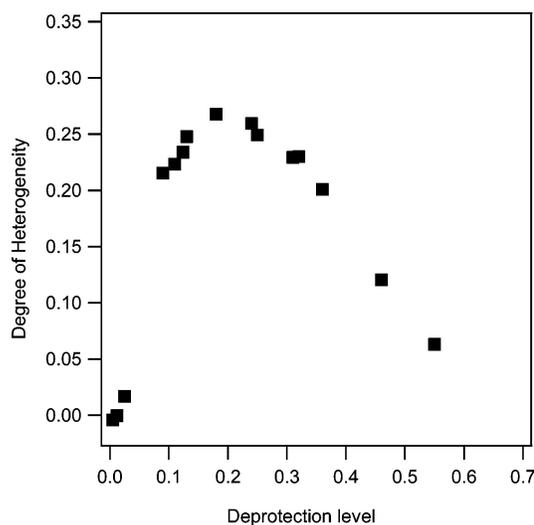
Figure 4. Degree of heterogeneity ($F_{bond} - 0.86\phi$) vs deprotection level in PMAdMA film for photoacid concentration $C = 0.006$ nm^{-3}.

can be expressed as the sum of the core (hydrogen bonded) and the shell (free), such that

$$V_{MAA} = V_c + A_s b \qquad (4)$$

The IR spectrum results from an ensemble of these deprotection volumes formed by individual photoacids. This average, ϕ, is related to the volume deprotected by a single photoacid and distance between photoacids. For a system with photoacid number concentration C, the average volume per photoacid (V_{PAG}) is $1/C$. For isolated deprotection regions:

$$\phi = V_{MAA}/V_{PAG} = (V_c + A_s b)C \qquad (5)$$

From eq 5, the deprotection volume can be estimated as a function of photoacid concentration and deprotection level. For a spherical deprotection volume, F_{bond} can be calculated as the fraction of hydrogen-bonded MAA within the core of the sphere to the total MAA. An efficiency factor, ϵ, is included to parametrize the fraction of MAA within the core that participates in hydrogen bonding. This factor is not expected to be unity because hydrogen-bonding depends upon the correct orientation of two carboxylic groups, may be composition dependent, and may not be static at the temperatures of the measurement (local dynamics), and the actual deprotection volume may not be a solid sphere.

$$F_{bond} = \frac{\epsilon V_c}{V_c + b A_s} = \frac{\epsilon}{1 + (A_s/V_c)b} = \frac{\epsilon}{1 + 3b/r} \qquad (6)$$

Equation 6 is used to fit the data in Figure 1b with the efficiency factor, ϵ, used as a fitting parameter. For the best fit to the data, we find that $\epsilon = 0.86$. By closely examining the data at low ϕ, it is clear that the model does not accurately predict the functional dependence of ϕ on F_{bond}. The spherical model predicts a more rapid increase in F_{bond} than is observed experimentally. One source of this discrepancy is the shape of the deprotection; we assumed a solid sphere geometry, but the actual deprotection path is more diffuse with incomplete deprotection.[22] This picture of the deprotection volume would result in less hydrogen bonding at equivalent ϕ in comparison to the solid sphere and would be more consistent with a homogeneous distribution around the photoacid. Also, a non-spherical core–shell geometry also has a higher surface to
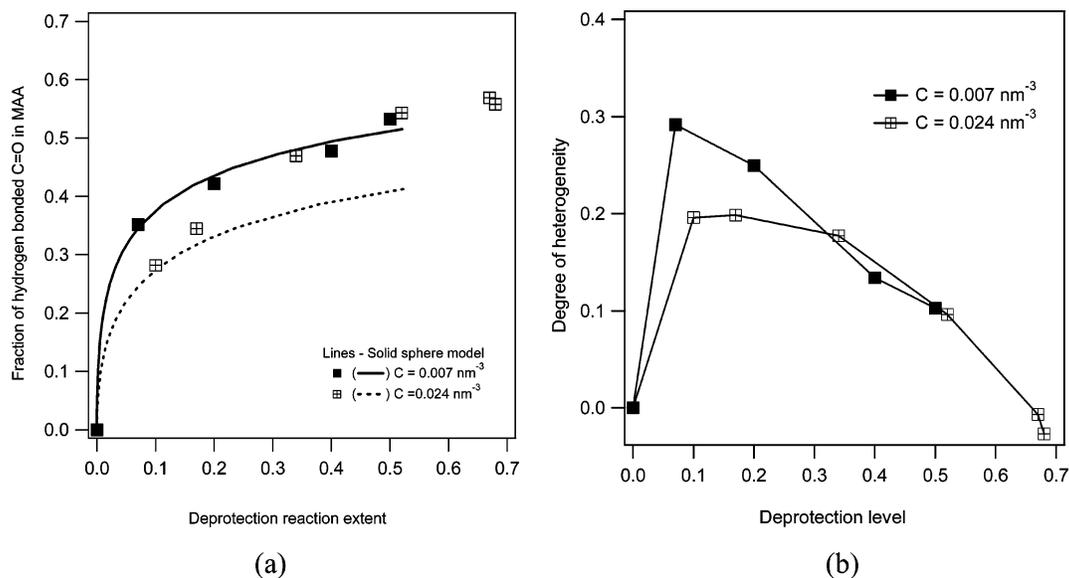
Figure 5. (a) Effect of acid concentration (C) on the fraction of hydrogen-bonded C=O (F_{bond}) in MAA for PMAdMA as a function of extent of deprotection (ϕ). (b) Degree of heterogeneity as a function of the deprotection extent of the film.
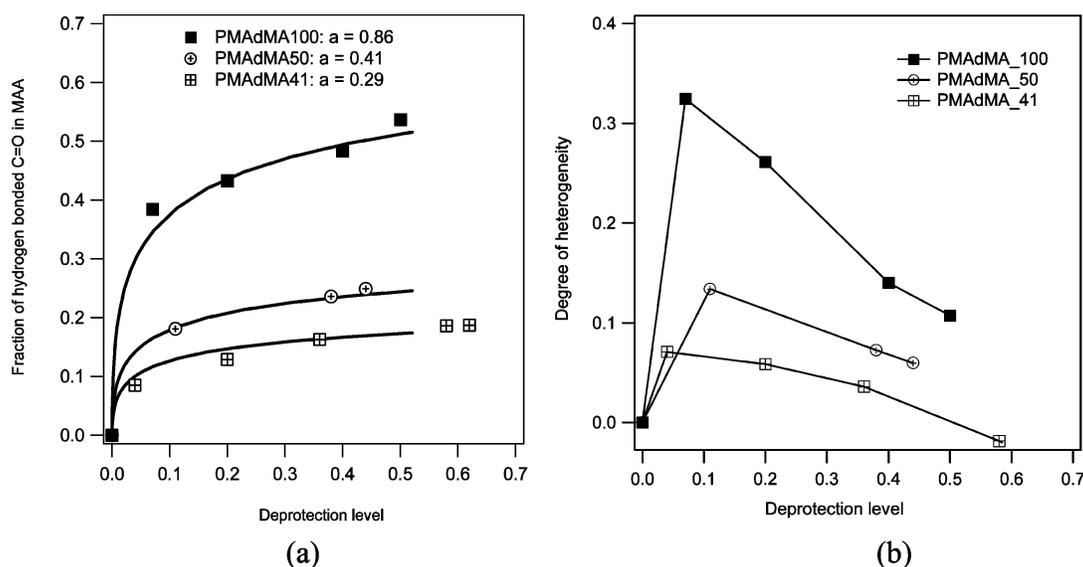
Figure 6. (a) Effect of comonomer composition on the hydrogen-bonded C=O fraction (F_{bond}) as a function of deprotection extent (ϕ). (b) Degree of heterogeneity vs deprotection extent. The photoacid concentration is 0.007 nm^{-3} for all samples.

volume ratio and would predict a lower fraction of hydrogen bonding, consistent with the deviation. At higher ϕ, the solid sphere model fails because the deprotection volumes from different photoacids will begin to overlap. The radius of the deprotection sphere can be simply calculated from the following equation:

$$4/3\pi R^3 C = \phi \tag{7}$$

The deprotection sphere radius in this study is found between 0.5 and 2.8 nm for an acid concentration $C = 0.006$ nm^{-3}. The condition of overlap occurs when the diameter of the deprotection spheres exceeds the mean intersphere distance. For a given acid concentration C, the criteria for sphere overlap is $R > \frac{1}{2}C^{-1/3}$, which corresponds to a deprotection level of 0.524.

3.4. Dependence of Heterogeneity on Deprotection Level. The fact that the efficiency factor, ϵ, is less than one confirms our expectation that the dimerization efficiency cannot be 100% for MAA pairs. Although the dimerization situation in a solid

sphere could be different from that in random distribution, we assume that the hydrogen-bonding efficiency for a physically adjacent MAA pair is constant, i.e., $\epsilon \approx 0.86$. However, it should be mentioned that the ϵ could be overestimated in this way because the dimerization for a MAA pair can come from all direction in a solid sphere while the chance for a MAA pair to dimerize in a diffuse volume is always less.

With this efficiency value, we can calculate the degree of heterogeneity (DH) and the dependence of DH on deprotection level as shown in Figure 4. It can be seen that the DH is small at very low and very high deprotection level, but is maximized at a deprotection level of approximately 0.20−0.25. These trends arise because the system heterogeneity is dominated by one component at low or high deprotection levels and the contrast from the uniform phase is small. It is interesting to note that the DH data are not symmetrical about the peak position. The reason for this behavior is not clear but could be related to the specific structure of the domains. The same reason could also

account for the data shown in Figure 2, in which the F_{bond} or DH follow almost a straight line with ϕ for polymer blends. The phase separation in these polymer blends could undergo a more complicated path such as that found in spinodal decomposition. Therefore, the MAA domains could take on more complicated shapes than the solid sphere model here and the number of domains may not be constant.

3.5. Dependence of Heterogeneity on Photoacid Concentration. The degree of heterogeneity depends upon changes in the photoacid concentration and can be expressed through eqs 5 and 6. Using the previous analysis of degree of heterogeneity and deprotection length scales, we examine the degree of heterogeneity for the same ϕ and different photoacid concentrations. Figure 5a shows the change in F_{bond} at two photoacid concentrations. At low ϕ, the degree of heterogeneity decreases for the larger photoacid concentration. If the deprotection is in the form of isolated spheres, increasing the number of spheres while maintaining a constant sphere volume (equivalently ϕ) requires smaller spheres, which increases the surface area to volume ratio. This point can also be illustrated by applying the solid sphere model using parameters determined previously in section 3.3 and only changing the acid concentration. The calculations are shown by the lines in Figure 5a. For low levels of deprotection ($\phi < 0.3$), the model reasonably fits the data at both acid concentrations. However at higher ϕ, F_{bond} becomes nearly independent of the photoacid concentration and the model no longer fits the data. Recall that one assumption of the model is that the deprotection volumes are isolated spheres, but at sufficient extents of deprotection the volumes will begin to overlap. This lack of photoacid concentration dependence on F_{bond} is expected when the deprotection volumes overlap significantly.

Figure 5b shows the degree of heterogeneity for the two different acid concentration systems. A larger heterogeneity occurs at lower deprotection levels for the lower photoacid concentration. From this result, we see that higher photoacid concentrations lead to lower heterogeneity, which correlates well with known effects observed for line-edge roughness. While the details of LER include the reaction and development steps, the latent-image quality does appear to correlate well with LER with a general consensus that the heterogeneity at the line-edge is a precursor to large physical roughness upon development.[10,13,29] From this analysis, the deprotection level that leads to the largest degree of heterogeneity can be measured with FTIR data. If the solubility composition limit for a deprotected resist lies near the deprotection level with the highest DH, this resist may have a higher LER than a resist where the solubility limit is higher or lower than the deprotection level of maximum DH. In the case of partially deprotected PMAdMA thin films the heterogeneity leads to dissolution regimes.[25] The onset to swelling and dissolution regimes are governed by the average film composition and percolation threshold of hydrophilic MAA groups. The ability to quantify and relate the heterogeneity to thin film development provides a step to compare materials with varying chemical functionality as well as composition.

3.6. Dependence of Heterogeneity on Comonomer Composition. Thus far, the discussion has focused on the deprotection of PMAdMA, a homopolymer. Many photoresists contain nonreactive monomers that provide additional functionality such as controlled dissolution or improved etch resistance.[1] Although it has been noted by photoresist researchers that introducing nonreactive comonomer in photoresist polymer can help improve the LER, the mechanism for this behavior is not well understood. It is interesting to examine how the degree of heterogeneity is

affected by the copolymer composition. Figure 6a shows F_{bond} changes with copolymer composition through the deprotection of copolymers containing 100%, 50%, and 41% MAdMA with a constant photoacid concentration and PEB temperature. The data are fitted to the solid sphere model and we can obtain an efficiency parameter for each copolymer composition. It is found that efficiency factor, ϵ, decreases monotonically with increasing GBLMA content of the copolymer. By normalizing the efficiency to the homopolymer, the value for ϵ is similar to the initial comonomer composition; normalized $\epsilon = 0.48$ for $f_{GBLMA} = 0.50$ and 0.34 for $f_{GBLMA} = 0.41$. This result shows that the hydrogen-bonding efficiency or dimerization efficiency is diluted by the GBLMA comonomer.

Figure 6b shows the degree of heterogeneity characterized by the deviation of F_{bond} from the reference line as a function of copolymer composition. Here, the reference line in eq 3 has been corrected by each copolymer composition because the deprotection level used here is a normalized number. It can be seen that the degree of heterogeneity consistently decreases with increasing GBLMA content. This decrease arises because the deprotection sphere contains more GBLMA and dilutes the overall MAA concentration such that the contrast with the protected regions become smaller, intrinsically resulting in a lower degree of heterogeneity.

4. Conclusion

The heterogeneous structures in partially deprotected photoresist polymer thin films have been characterized with FTIR with quantification of the degree of heterogeneity through the fraction of hydrogen-bonded carboxyl groups. The degree of heterogeneity depends on the extent of reaction, acid concentration, and comonomer composition. The heterogeneity occurs initially due to discrete domain volumes formed by the photoacid catalyzed reaction within the polymer matrix. Deviations from a solid sphere model occur due to overlap of the deprotection volumes from multiple photoacids and fractal nature (nonspherical) of the true deprotection volume. This work has established an experimental method to quantify the degree of heterogeneity in hydrogen-bonded thin films. The deviation from a reference state of heterogeneity (homogeneous mixture) permits different systems to be compared quantitatively. We expect that the degree of heterogeneity within complex systems such as gels in bulk or thin film form can benefit from this approach and complement other methods such as small-angle neutron scattering to quantify and characterize the structure of heterogeneous systems.

References and Notes

(1) Ito, H. *Adv. Polym. Sci.* **2005**, *172*, 37−245.
(2) Willson, C.; Ito, H.; Frechet, J.; Tessier, T.; Houliham, F. *J. Electrochem. Soc.* **1986**, *133* (1), 181−187.
(3) Ito, H. *J. Polym. Sci. Part A: Polym. Chem.* **2003**, *41*, 3863−3870.
(4) Reichmanis, E.; Nalamasu, O.; Houlihan, F. M.; Novembre, A. E. *Polym. Int.* **1999**, *48*, 1053−1059.
(5) Hinsberg, W.; Houle, F. A.; Hoffnagle, J.; Sanchez, M.; Wallraff, G.; Morrison, M.; Frank, S. *J. Vac. Sci. Technol. B* **1998**, *16*, 3689−3694.
(6) Levinson, H. J.; Arnold, W. H. *J. Vac. Sci. Technol. B* **1987**, *5*, 293−298.
(7) Pawloski, A.; Acheta, A.; Lalovic, I.; La Fontaine, B.; Levinson, H. *Proc. SPIE−Int. Soc. Opt. Eng.* **2004**, *5376* (1), 414−425.
(8) Vogt, B. D.; Kang, S.; Prabhu, V. M.; Lin, E. K.; Satija, S. K.; Turnquest, K.; Wu, W. *Macromolecules* **2006**, *39*, 8311−8317.
(9) Vogt, B. D.; Kang, S.; Prabhu, V. M.; Rao, A.; Lin, E. K.; Wu, W. L.; Satija, S. K.; Turnquest, K. *J. Vac. Sci. Technol. B* **2006**, *25*, 175−182.
(10) Schmid, G. M.; Stewart, M. D.; Singh, V. K.; Willson, C. G. *J. Vac. Sci. Technol. B* **2002**, *20*, 185−190.

(11) Schmid, G. M.; Stewart, M. D.; Burns, S. D.; Willson, C. G. *J. Electrochem. Soc.* **2004**, *151* (2), G155−G161.

(12) Flanagin, L. W.; Singh, V. K.; Willson, C. G. *J. Vac. Sci. Technol. B* **1999**, *17*, 1371−1379.

(13) Houle, F. A.; Hinsberg, W. D.; Sanchez, M. I.; Hoffnagle, J. A. *J. Vac. Sci. Technol. B* **2002**, *20*, 924−931.

(14) Houle, F. A.; Hinsberg, W. D.; Sanchez, M. I. *J. Vac. Sci. Technol. B* **2004**, *22*, 747−757.

(15) Sarris, V.; Patsis, G. P.; Constantoudis, V.; Boudouvis, A. G.; Gogolides, E. *Jpn. J. Appl. Phys. Part 1: Reg. Pap. Brief Commun. Rev. Pap.* **2005**, *44*, 7400−7403.

(16) Patsis, G. P.; Gogolides, E. *J. Vac. Sci. Technol. B* **2005**, *23*, 1371−1375.

(17) Ma, Y. S.; Shin, J.; Cerrina, F. *J. Vac. Sci. Technol. B* **2003**, *21*, 112−117.

(18) Yamaguchi, A.; Takahashi, M.; Kishimura, S.; Matsuzawa, N.; Ohfuji, T.; Tanaka, T.; Tagawa, S.; Sasago, M. *Jpn. J. Appl. Phys. Part 1: Reg. Pap. Short Notes Rev. Pap.* **1999**, *38* (7A), 4033−4040.

(19) Tsiartas, P. C.; Flanagin, L. W.; Henderson, C. L.; Hinsberg, W. D.; Sanchez, I. C.; Bonnecaze, R. T.; Willson, C. G. *Macromolecules* **1997**, *30*, 4656−4664.

(20) Stewart, M. D.; Somervell, M. H.; Tran, H. V.; Postnikov, S. V.; Willson, C. G. *Proc. SPIE: Int. Soc. Opt. Eng.* **2000**, *3999*, 665−674.

(21) Dragnea, B.; Preusser, J.; Schade, W.; Leone, S.; Hinsberg, W. *J. Appl. Phys.* **1999**, *86*, 2795−2799.

(22) Jones, R. L.; Hu, T. J.; Lin, E. K.; Wu, W. L.; Goldfarb, D. L.; Angelopoulos, M.; Trinque, B. C.; Schmid, G. M.; Stewart, M. D.; Willson, C. G. *J. Polym. Sci., Part B: Polym. Phys.* **2004**, *42*, 3063−3069.

(23) Higashi, N.; Matsumoto, T.; Niwa, M. *Langmuir* **1994**, *10*, 4651−4656.

(24) Lee, J. Y.; Painter, P. C.; Coleman, M. M. *Macromolecules* **1988**, *21*, 346−354.

(25) Rao, A.; Kang, S.; Vogt, B. D.; Prabhu, V. M.; Lin, E. K.; Wu, W. L.; Muthukumar, M. *Langmuir* **2006**, *22*, 10009−10015.

(26) Kang, S.; Prabhu, V. M.; Vogt, B. D.; Lin, E. K.; Wu, W. L.; Turnquest, K. *Polymer* **2006**, *47*, 6293−6302.

(27) Higashi, N.; Matsumoto, T.; Niwa, M. *Langmuir* **1994**, *10*, 4651−4656.

(28) Desiraju, G.; Steiner, T. *The Weak Hydrogen Bond;* Oxford University Press: New York, 1999.

(29) Pawloski, A.; Acheta, A.; Levinson, H.; Michaelson, T. B.; Jamieson, A.; Nishimura, Y.; Willson, C. G. *J. Microlith., Microfab., Microsyst.* **2006**, *5* (2), 023001-1.−023001-16.